August 2004 • NREL/CP-520-36747

Conference Paper

A Review and Understanding of Screen-Printed Contacts and Selective–Emitter Formation

Preprint

M.M. Hilali and A. Rohatgi
Georgia Institute of Technology

B. To
National Renewable Energy Laboratory

To be presented at the 14th Workshop on Crystalline Silicon Solar Cells and Modules
Winter Park, Colorado
August 8-11, 2004

National Renewable Energy Laboratory
1617 Cole Boulevard, Golden, Colorado 80401-3393
303-275-3000 • www.nrel.gov

Operated for the U.S. Department of Energy
Office of Energy Efficiency and Renewable Energy
by Midwest Research Institute • Battelle

Contract No. DE-AC36-99-GO10337

Available electronically at http://www.osti.gov/bridge

Available for a processing fee to U.S. Department of Energy and its contractors, in paper, from:

U.S. Department of Energy
Office of Scientific and Technical Information
P.O. Box 62
Oak Ridge, TN 37831-0062
phone: 865.576.8401
fax: 865.576.5728
email: mailto:reports@adonis.osti.gov

Available for sale to the public, in paper, from:

U.S. Department of Commerce
National Technical Information Service
5285 Port Royal Road
Springfield, VA 22161
phone: 800.553.6847
fax: 703.605.6900
email: orders@ntis.fedworld.gov
online ordering: http://www.ntis.gov/ordering.htm

Printed on paper containing at least 50% wastepaper, including 20% postconsumer waste

A Review and Understanding of Screen-Printed Contacts and Selective–Emitter Formation

Mohamed M. Hilali[1], Bobby To[2], Ajeet Rohatgi[1]
[1]University Center of Excellence for Photovoltaics Research and Education
School of Electrical and Computer Engineering
Georgia Institute of Technology, Atlanta, GA 30332-0250
[2]National Renewable Energy Laboratory, Golden, CO 80401

Abstract

A comparison of the loss mechanisms in screen-printed solar cells relative to buried contact cells and cells with photolithography-defined contacts is presented in this paper. Model calculations show that emitter recombination accounts for about 0.5% absolute efficiency loss in conventional screen-printed cells with low-sheet-resistance emitters. Ohmic contact to high-sheet-resistance emitters by screen-printing has been investigated to regain this efficiency loss. Our work shows that good quality ohmic contacts to high sheet-resistance emitters can be achieved if the glass frit chemistry and Ag particle size are carefully tailored. The melting characteristics of the glass frit determine the firing scheme suitable for low contact resistance and high fill factors. In addition, small to regular Ag particles were found to help achieve a higher open-circuit voltage and maintain a low contact resistance. This work has resulted in cells with high fill factors (0.782) on high sheet-resistance emitters and efficiencies of 17.4% on planar float zone Si substrates, without the need for a selective emitter.

Introduction

Solar cell metallization is a major efficiency-limiting and cost-determining step in solar cell processing [1]. Screen-printed (SP) metallization is the most widely used contact formation technique for commercial Si solar cells [2, 3]. Photolithography (PL) and metal evaporation is the most well-established metallization technique for solar cell fabrication. In this technique, the metal contact resistance is normally very low (1×10^{-5} mΩ-cm^2) [4] with very narrow gridlines (~8 μm) and virtually no junction shunting, resulting in the highest fill factors and cell performance. World record efficiencies of 24.7% on single crystal Si [5] and 20.3% on cast multicrystalline Si [6] have been achieved with PL contacts. However, this technology is time-consuming and expensive due to the use of photo-resist mask patterning and vacuum evaporation of metals. This has lead to the development and use of simpler metallization techniques in production. The buried-contact (BC) technology was developed at the University of New South Wales to produce fine lines, obtain high aspect ratios, and achieve good metal-conductivity and low contact-resistance [7]. This technology also allows for the formation of a selective-emitter or a lightly doped emitter region between the grooves, lowering the surface recombination and enhancing the blue response. The use of Ni/Cu contacts reduces the cost of materials compared to the cost of Ag contacts in the SP cells. However, the BC module is ~\$0.38/W higher than the SP module [1]. Screen-printed contact technology is a more rapid metallization process and cost-effective compared to PL and BC technologies. The screen-printing equipment is robust, simple, and inexpensive and the technique can be easily automated. It produces less chemical waste with little environmental impact, and is modular for actual production facilities [9].

Screen-printing is truly a cost-effective option for large-scale solar cell manufacturing provided that high-quality contacts with FF≥0.77 can be achieved in production.

An understanding of the loss mechanisms in screen-printed contacts

Factors that tend to limit the solar cell performance of screen-printed cells are summarized below:

- Screen-printed contacts are typically 125-150 μm wide, which gives rise to high shading losses.
- Fill factors are low (~0.75) because of high contact resistance, low metal conductivity, and junction shunting.
- Effective emitter surface passivation is difficult because of the use of low sheet-resistance emitters with a high surface concentration. This is done to achieve a reasonable contact resistance (≤ 3 mΩ-cm^2). This also results in poor short-wavelength response due to heavy doping effects and increased Auger recombination in the emitter region.

Due to the above factors, the efficiency of screen-printed cells is typically 1.5-2% lower than that of cells with photolithography contacts [10]. Model calculations in Fig. 1 show the quantitative breakdown of these losses, which are divided into three categories: contact quality, short-wavelength response, and shading. The pie chart in Fig. 1 shows that contact quality is inferior due to high contact-resistance, low conductivity of the SP Ag gridline, and emitter sheet resistance loss due to wider gridline spacing. The loss in short-wavelength response is caused by a high front-surface recombination velocity and heavy-doping effects in the emitter. Finally, the high shading loss is due to the wide SP gridline and busbar. Table 1 summarizes the key differences in contact parameters and quality of PL, BC, and SP contacts.

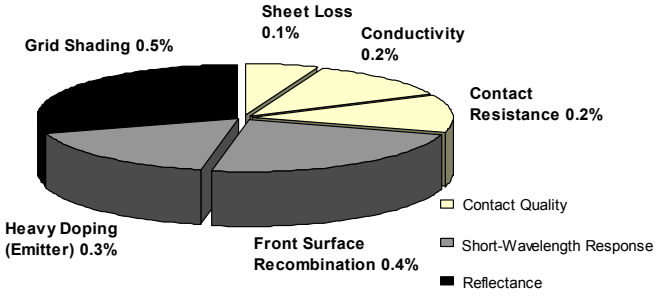

Fig. 1. Loss mechanisms in SP cells relative to PL cells.

Table 1: A comparison of SP, BC, and PL front contact metallization techniques.

Parameter	SP Cell	BC cell	PL cell
finger thickness	14 μm	50 μm	8 μm
finger width	80 μm	20 μm	20 μm
specific contact-resistance	0.3-3 mΩ-cm^2	3 μΩ-cm^2	0.01 mΩ–cm^2
metal resistivity	3 μΩ-cm	1.7 μΩ-cm	1.7 μΩ-cm
Fill Factor	0.74-0.77	0.78-0.79	0.81-0.82

Selective-Emitter Cells

The advantages of a selective-emitter cell include a low contact resistance due to heavy doping underneath the metal grid, improved front-surface passivation of the lightly doped region between the grid, and reduced recombination under the metal contact. In the case of BC cells a selective-emitter is achieved by two-step diffusion with the heavy diffusion only in the grooves. Therefore, the BC cell can be categorized as a selective-emitter cell with plated contacts [11].

In the case of screen-printing, a selective-emitter is difficult to achieve especially by a one-step process. Recently several innovative techniques to form a screen-printed selective-emitter cell have been attempted. These techniques can be divided in three categories:

(a) selective-emitter cells fabricated via masking and etching with no alignment [12],
(b) selective-emitter cells fabricated by self-alignment without the need for masking or etching [13], and
(c) selective-emitter cells fabricated by self-aligned self-doping Ag pastes [14, 15].

Techniques (a) and (b) are generally time consuming and somewhat expensive. Technique (c) is not trivial because the diffusivity of Ag in Si [16] is higher than that of P [17], which can lead to a high junction leakage current and n factor. To develop screen-printed contacts to high sheet resistance emitters, we first review the current understanding of screen-printed formation. Then we discuss our work on the formation of good SP ohmic contacts to high sheet-resistance emitters. This work has resulted in cells with high fill factors (0.782) and efficiencies of 17.4% on untextured FZ Si substrates, without the need for a selective emitter.

A Brief Review of the Current Understanding of the Contact Formation and Current Transport Through Screen Printed Contacts

Screen-printed contact formation and current transport is not fully understood, nevertheless, Ballif et al. [18,19] and Schubert et al. [20-22] have proposed some models based on electrical and physical characterization of screen-printed contacts. The glass frit included in commercial Ag pastes plays a crucial role in contact formation. Lead borosilicate glass frit is commonly used, which etches the antireflection coating, reduces the melting point of Ag, and promotes adhesion to Si during the firing cycle. The reaction between the glass frit and the SiN_x layer takes place via a redox reaction [23]. The glass frit also acts as a barrier to Ag diffusion from the paste into the emitter region and p-n junction [24]. This could help in reducing junction shunting and leakage current.

The general understanding is that upon heating the glass frit melts and wets the surface. According to the Pb-Ag phase diagram, the glass frit dissolves Ag and etches the SiN_x antireflection coating while the Ag is sintered during firing. When the liquid glass reaches the Si emitter, Si is also dissolved in the lead-silver melt. Upon cooling, Si re-grows epitaxially [18, 25, 26] followed by Ag crystallites at the Si surface. The glass layer then solidifies and Pb precipitates are formed in the glass layer. The Ag crystallites are believed to be isolated metal-semiconductor ohmic contact regions responsible for the current transport from the Si emitter to the Ag grid, and have very low contact resistivity (2×10^{-7} Ω-cm^2) with the Si emitter [19]. In some cases the Ag crystallites at the Si emitter surface re-crystallize along (111) planes to give an inverted pyramid shape. However, sometimes the Ag crystallites are elongated or form a rounded interface with the Si

emitter depending on the glass-Ag-Si interaction. Figure 2 shows a SEM image of the Ag-Si interface and the re-grown Ag crystallites. As shown in Fig. 3, current transport can take place by three possible methods: direct interconnection at isolated spots between the Ag crystallites and the Ag grid [26, 27], tunneling through ultra-thin glass regions [19] as shown in Fig. 3(a), and conduction through the glass layer by tunneling via discontinuous metal granules in the glass layer [28, 29] (Fig. 3(b)).

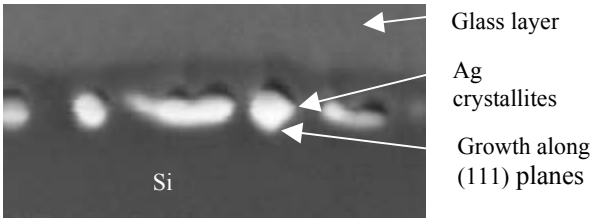

Fig. 2. SEM image of Ag crystallites at the Ag-Si interface.

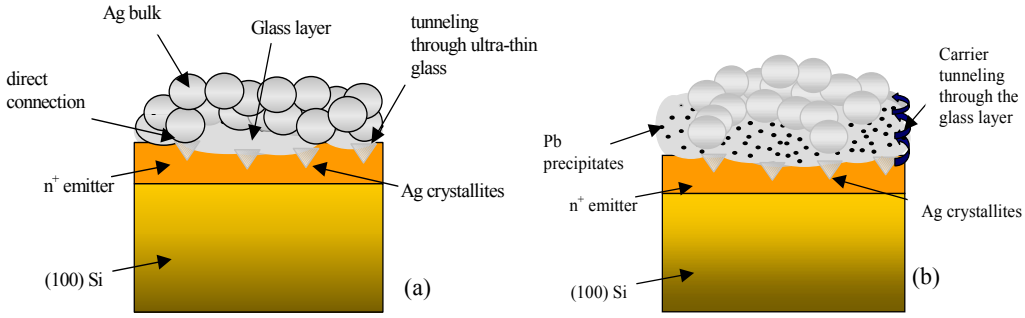

Fig. 3. Current transport from the Si emitter to the Ag grid via (a) direct connection between Ag crystallites and Ag bulk, tunneling through ultra-thin glass regions, and (b) conduction within the glass layer via tunneling between metal precipitates.

Challenges for Contact Formation on High Sheet-Resistance Emitter

An alternative technique to the selective-emitter is to optimize the paste and firing conditions to achieve high-quality contacts on the lightly doped emitters with shallow junctions [30, 31]. Optimization of contact firing should result in low contact-resistance, while maintaining a high open-circuit voltage [32]. This is a real challenge because the glass frit in the paste needs to be formulated carefully so as to selectively etch the SiN_x layer without shunting the shallow p-n junction. The other challenge is to form a good ohmic contact between the Ag and Si emitter, which has a lower P doping, resulting in higher specific-contact-resistance based on the tunneling process described by the following equation [33]:

$$\rho_c = \exp\left(\frac{2\sqrt{\varepsilon_s m^*}}{\hbar}\left(\frac{\phi_{Bn}}{\sqrt{N_D}}\right)\right),$$

where N_D is the doping concentration ($\geq 10^{19}$ cm^{-3}), m^* is the effective mass of the charge carriers, ε_s is the semiconductor permittivity, $\hbar$ is the reduced Planck constant, and ϕ_B is the Schottky barrier height. The surface doping for both the 45 and 100 Ω/sq emitters used in our cell process is greater than 10^{19} cm^{-3}, however, the high sheet-resistance emitter is shallower (0.277 μm) than the low sheet-resistance emitter (0.495 μm). Hence, a key technology is to achieve good ohmic contacts without degrading or shunting the p-n junction. This requires an optimization of the glass frit, Ag powder in the paste and contact firing.

Criteria for the Glass frit Behavior to Achieve High-Quality Contacts to High Sheet-Resistance Emitters

Aggressive glass frit etches more Si and allows the dissolved Ag to penetrate deep into the p-n junction. Excessive penetration of Ag in the emitter region can also occur if the glass layer does not properly act as a barrier to Ag diffusion. Figure 4 shows SIMS Ag profiles in the Si emitter region underneath the Ag gridline for an aggressive glass and a mild glass that is designed to prevent Ag diffusion into the Si emitter. Excessive penetration of Ag into the p-n junction region degrades V_{oc} [34] due to an increase in the junction leakage current (J_{o2}) [30]. Suns-V_{oc} analysis [35] showed that J_{o2} is very high (2,678 nA/cm^2) for the aggressive glass frit in Fig. 4, and is lower (15 nA/cm^2, n_2=2) for the less aggressive glass frit.

To achieve good ohmic contact to a high sheet-resistance emitter without shunting the shallow emitter, the glass frit must not be very aggressive. However, if the glass frit is very mild, it will not etch the SiN_x completely for conventional firing temperatures. For example, we have found that inadequate firing of PV168 Ag paste from Dupont led to a very high specific contact-resistance (46 mΩ-cm^2). A more aggressive etching reaction between the glass frit and the SiN_x was achieved by firing at higher temperatures (>810°C). This caused the SiN_x layer to be etched and resulted in Ag crystallite re-growth on the Si emitter surface. As a result, the specific contact-resistance decreased significantly to ≤2 mΩ-cm^2.

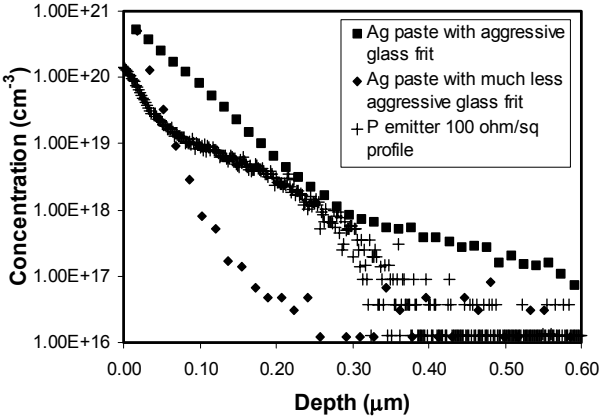

Fig. 4. SIMS Ag profiles for aggressive and mild glass frit.

As reported in [19], a problem in contacting lightly doped emitters is the sparse contact regions (Ag crystallites) between the Si emitter and the Ag grid. Atomic force microscopy (AFM) can be used to obtain a footprint of the distribution of the Ag crystallites at the Ag-Si interface for different Ag pastes. Figure 5 shows AFM plane-view images of two Ag pastes after removal of the Ag and glass frit; one shows (a) sparse irregular pit distribution and higher ρ_c ~3 mΩ-cm^2 and the other (b) shows a more regular and uniform distribution of pits or inverted pyramids and lower ρ_c ~0.6 mΩ-cm^2. It was found that glass frit with a lower glass transition temperature (T_g) helps improve the formation of a large number of Ag crystallites at the Si emitter surface and increases their size.

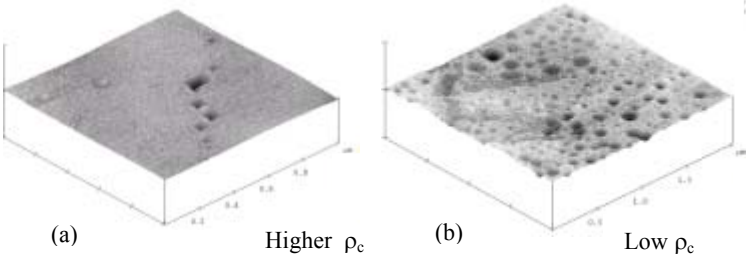

Fig. 5. AFM plane-view images for (a) sparsely distributed, and (b) regularly distributed Ag crystallites after the removal of the Ag and glass frit contact.

Criteria for Contact Firing

In addition to optimizing the glass frit, the firing profile also must be optimized to control the thickness of the glass layer between the Si emitter and the Ag. We have found that high temperature firing and long dwell times cause more glass frit to seep between the Ag bulk and the Si emitter. Rapid firing of screen-printed contacts could be useful in achieving a lower contact resistance because it allows the glass frit to etch the SiN_x without shunting the Si emitter. Fast firing could also prevent the formation of a thick glass layer between the Ag grid and the Ag crystallites at the Si emitter surface.

Criteria for Ag Particles

The Ag particle size is an important factor that influences the contact resistance. We observed that ultra-fine Ag particles allow a thick and more uniform glass layer to form between the Si emitter and Ag grid (Fig. 6(a)). On the other hand, we observed a non-uniform glass layer that is very thin in some regions when large Ag particles are used. Figure 6(b) shows that for larger Ag particle size, regions where Ag is in direct or very close contact to the Si emitter are more frequent. This results in a low ρ_c but also it causes a decrease in V_{oc} by 7 mV and a rise in the n factor (>1.2). The decrease in V_{oc} because of larger Ag particle size in the paste may be due to the higher surface-recombination at the metal surface, which is in direct contact with the emitter in many regions. However, solar cells made using an Ag paste with ultra-fine particles results in a higher V_{oc} of 643 mV as well as higher ρ_c due to the thicker glass layer in the Ag-Si contact. Thus, we have found that small- to medium-sized Ag particles are optimum for achieving acceptably low specific contact-resistance (~1 mΩ-cm^2) while maintaining a high V_{oc} (~641 mV).

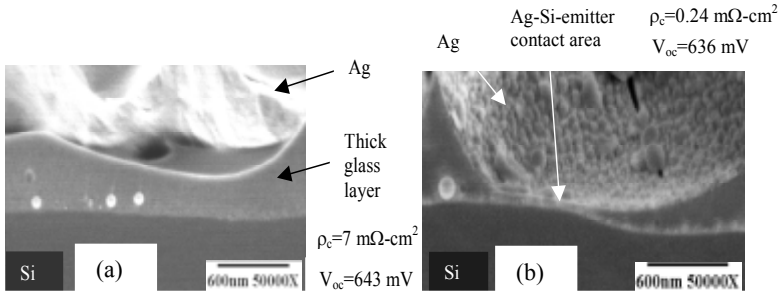

Fig. 6. SEM images of Ag-Si interface with (a) thick glass layer for ultra-fine Ag particle size in the paste, and (b) Ag-Si emitter contact for large Ag particle size.

High-Efficiency Cells on 100 Ω/sq Emitters

We have achieved untextured FZ cell efficiencies as high as 17.4% on a 100 Ω/sq emitter. However, sometimes there is a slight scatter or non-uniformity in cells made on the 100 Ω/sq emitter. Fill factors are generally higher for the 40 Ω/sq-emitter cells because of the lower sheet-resistance loss. When good ohmic contact is achieved on 90-100 Ω/sq emitters, an improvement of ~0.2-0.4% in absolute efficiency is observed over the ~40 Ω/sq emitter. Tables 2 and 3 show the best and average cell efficiencies achieved on 100 and 40 Ω/sq emitters using the Ferro paste 33-462.

Table 2: 90-100 Ω/sq-emitter cells using paste 33-462.

Cell Name	V_{oc} (mV)	J_{sc} (mA/cm^2)	FF	Eff (%)	n factor	R_s (Ω-cm^2)	R_{sh} (Ω-cm^2)
Best Cell	642	34.31	0.786	17.32	1.03	0.948	27725
Average	640	34.34	0.773	17.00	1.12	0.553	233546
Standard Dev.	1	0.16	0.009	0.23	0.03	0.162	599234

Table 3: 40 Ω/sq-emitter cells using paste 33-462.

Cell Name	V_{oc} (mV)	J_{sc} (mA/cm²)	FF	Eff (%)	n factor	R_s (Ω-cm²)	R_{sh} (Ω-cm²)
Best Cell	638	33.66	0.797	17.1	1.03	0.592	94677
Average	637	33.50	0.790	16.87	1.05	0.719	50409
Standard Dev.	1	0.13	0.010	0.22	0.02	0.168	79500

Conclusions

It is desirable to find innovative metallization techniques to improve the cell efficiency without significantly increasing the cost. The fabrication of high quality screen-printed contacts on lightly doped emitters using a single-step co-firing process is in line with this goal. But many challenges remain before high-quality thick-film contacts to high sheet-resistance emitters become widespread in commercial PV cells. To achieve robust and high performance screen-printed contacts the glass frit content and chemistry must be optimized along with the firing conditions.

Our results show that both glass frit chemistry and Ag particle size are important for achieving good quality ohmic contacts to high sheet-resistance emitters. The melting characteristics of the glass frit determine the firing scheme suitable for low contact-resistance and high fill factors (FFs). In addition, small to regular Ag particles were found to help achieve a higher open-circuit voltage (V_{oc}) and maintaining a low contact resistance. P self-doping from the paste was not necessary for good contacts to high sheet-resistance emitters for the rapid firing schemes in this paper. High FFs (>0.78) were achieved on untextured FZ Si cells using rapid firing in a lamp-heated belt-furnace with efficiencies of up to 17.4% on a 100 Ω/sq emitter. This corresponds to an efficiency improvement of ~0.3% absolute over the 45 Ω/sq emitter cells.

Acknowledgements

The authors would like to thank Dr. Sally Asher at NREL for SIMS measurements. The authors also wish to thank Dr. Vijay Yelundur for his assistance in preparing this manuscript.

References

[1] J. H. Wohlgemuth, S. Narayanan, and R. Brenneman, *Proc. 21st IEEE PVSC, 221-226* (1990).
[2] J. F. Nijs, J. Sclufcik, J. Poortmans, S. Sivoththaman, and R. P. Mertens, *IEEE Trans. on Elect. Dev.* **46**, 1948-1969 (1999).
[3] G. Schubert, F. Huster, and P. Fath, *PVSEC-14*, , 441-442 (2003).
[4] D. L. Meier and D. K. Schroder, *IEEE Trans. on Elect. Dev.* **31**, 647-653 (1984).
[5] J. Zhao, A. Wang, M. A. Green, *Sol. Energy Mater. and Sol. Cells* **66**, 27-36 (2001).
[6] O. Schultz, S.W. Glunz, *19th EU PVSEC*, (2004) in press.
[7] S. Wenham, *Prog. in Photovoltaics,* **1**, 3-10 (1993).
[8] D. Jordan and J. P. Nagle, *Prog. in Photovoltaics,* **2**, 171-176 (1994).
[9] L. Frisson, G. Cheek, R. Mertens, and R. Van Overstraeten, *Commission Eur. Commun. Report. EUR*, 1002-1006 (1984).
[10] P. Doshi, J. Mejia, K. Tate, and A. Rohatgi, *IEEE Trans. on Elect.Dev.* **44**, 1417-1424 (1997).

[11] T. Bruton, N. Mason, S. Roberts, O. N. Hartley, S. Gledhill, J. Fernandez, R. Russel, W. Warta, S. Glunz, O. Schultz, M. Hermle, and G. Wileke, *WCPEC-3* (2003).
[12] D. S. Ruby, P. Yang, M. Roy, and S. Narayanan, *Proc. 26th IEEE PVSC,* 39-42 *(*1997).
[13] J. Horzel, J. Szlufcik, J. Nijs, and R. Mertens, *Proc. 26th IEEE PVSC,* 139-142 (1997).
[14] A. Rohatgi, M. Hilali, D. L. Meier, A. Ebong, C. Honsberg, A. F. Carroll, and P. Hacke, *Proc. 17thEU PVSEC,* 1307-1310 (2001).
[15] L. M. Porter, A. Teicher, and D. L. Meier, *Sol. Energy Mater. and Sol. Cells* **73**, 209-219 (2002).
[16] F. Rollert, N. A. Stolwijk, and H. Mehrer, *J. Phys. D* **20**, 1148-1155 (1987).
[17] S. A. Campbell, *The Science and Engineering of Microelectronic Fabrication*, Oxford University Press: New York (1996).
[18] C. Ballif, D. M. Huljić, A. Hessler-Wysser, and G. Willeke, *Proc. 29th IEEE PVSC*, 360-363 (2002).
[19] C. Ballif, D. M. Huljić, G. Willeke, and A. Hessler-Wysser, *Appl. Phys. Lett*. **82**, 1878-1880, (2003).
[20] G. Schubert, F. Huster, and P. Fath, *19th EU PVSEC*, (2004) in press.
[21] G. Schubert, B. Fischer, and P. Fath, *Photovolt. in Europe Conf.*, Rome, (2002).
[22] G. Schubert, F. Huster, ad P. Fath, *PVSEC-14*, (2004) pp. 441-442.
[23] R. J. S. Young and Alan F. Carroll, *Proc.16th EU PVSEC,* 1731-1734 (2000).
[24] A. Shaikh, S. Sridharan, T. Pham, and C. Khadilkar, *3rd WCPEC*, (2003).
[25] R. Mertens, M. Eyckmans, G. Cheek, M. Honore, and R. Van Overstraten, *Proc. 17th IEEE PVSC*, 1347-1351 (1984).
[26] G. C. Cheek, R. P. Mertens, R. Van Overstraeten, and L. Frisson, *IEEE Trans. on Elect. Dev.* **31**, 602-609 (1984).
[27] K. Firor, S. J. Hogan, J. M. Barrett, and R. T. Coyle, *Proc.16th IEEE PVSC*, 824-827(1982).
[28] O Growski, L. Murawski, and K. Trzebiatowsky, *J. Phys. D: Appl. Phys.* **15,** 1097-1101 (1982).
[29] T. Nakajima, A. Kawakami, and A. Tada, *Internat. J. of Hybrid Microelect.* **6**, 580-586 (1983).
[30] M. M. Hilali, A. Rohatgi, and S. Asher, *IEEE Trans. on Elect. Dev.,* **51**, 948-955 (2004).
[31] M. Bähr, S. Dauwe, L. Mittelstädt, J. Schmidt and G. Gobsch, 19th *EU PVSEC, (*2004) in press.
[32] H. H. C. de Moor, A. W. Weeber, J. Hoornstra, and W. C. Sinke, *6th Workshop on Cryst. Si Sol. Cell Mater. and Processes*, 154-170 (1996).
[33] S. M. Sze, *Physics of Semiconductor Devices*, 2nd ed. John Wiley & Sons: New York (1981).
[34] M. Van Craen, L. Frisson, and F. C. Adams, *Surface and Interface Analysis* **6**, 257-260 (1984).
[35] R. A. Sinton and A. Cuevas, *Proc. of the 16th EU PVSEC* **II,** 1152-1155 (2000).

REPORT DOCUMENTATION PAGE

Form Approved
OMB No. 0704-0188

PLEASE DO NOT RETURN YOUR FORM TO THE ABOVE ORGANIZATION.

1. REPORT DATE *(DD-MM-YYYY)*	2. REPORT TYPE	3. DATES COVERED *(From - To)*
August 2004	Conference Paper	

4. TITLE AND SUBTITLE
A Review and Understanding of Screen-Printed Contacts and Selective-Emitter Formation: Preprint

5a. CONTRACT NUMBER
DE-AC36-99-GO10337

5b. GRANT NUMBER

5c. PROGRAM ELEMENT NUMBER

6. AUTHOR(S)
M.M. Hilali and A. Rohatgi: Georgia Institute of Technology
B. To: NREL

5d. PROJECT NUMBER
NREL/CP-520-36747

5e. TASK NUMBER
PVP4.3001

5f. WORK UNIT NUMBER

7. PERFORMING ORGANIZATION NAME(S) AND ADDRESS(ES)
National Renewable Energy Laboratory
1617 Cole Blvd.
Golden, CO 80401-3393

8. PERFORMING ORGANIZATION REPORT NUMBER
NREL/CP-520-36747

9. SPONSORING/MONITORING AGENCY NAME(S) AND ADDRESS(ES)

10. SPONSOR/MONITOR'S ACRONYM(S)
NREL

11. SPONSORING/MONITORING AGENCY REPORT NUMBER

12. DISTRIBUTION AVAILABILITY STATEMENT
National Technical Information Service
U.S. Department of Commerce
5285 Port Royal Road
Springfield, VA 22161

13. SUPPLEMENTARY NOTES

14. ABSTRACT *(Maximum 200 Words)*

A comparison of the loss mechanisms in screen-printed solar cells relative to buried contact cells and cells with photolithography-defined contacts is presented in this paper. Model calculations show that emitter recombination accounts for about 0.5% absolute efficiency loss in conventional screen-printed cells with low-sheet-resistance emitters. Ohmic contact to high-sheet-resistance emitters by screen-printing has been investigated to regain this efficiency loss. Our work shows that good quality ohmic contacts to high sheet-resistance emitters can be achieved if the glass frit chemistry and Ag particle size are carefully tailored. The melting characteristics of the glass frit determine the firing scheme suitable for low contact resistance and high fill factors. In addition, small to regular Ag particles were found to help achieve a higher open-circuit voltage and maintain a low contact resistance. This work has resulted in cells with high fill factors (0.782) on high sheet-resistance emitters and efficiencies of 17.4% on planar float zone Si substrates, without the need for a selective emitter.

15. SUBJECT TERMS
PV; photovoltaics; solar cells; crystalline silicon; materials and processes; module; impurities; device process; crystal growth; defect; passivation; microelectronics

16. SECURITY CLASSIFICATION OF:			17. LIMITATION OF ABSTRACT	18. NUMBER OF PAGES	19a. NAME OF RESPONSIBLE PERSON
a. REPORT	b. ABSTRACT	c. THIS PAGE			
Unclassified	Unclassified	Unclassified	UL		19b. TELEPONE NUMBER (*Include area code)*